Journal of the European Ceramic Society xxx (xxxx) xxx

Contents lists available at ScienceDirect

Journal of the European Ceramic Society

journal homepage: www.elsevier.com/locate/jeurceramsoc

Processing and micro-mechanical characterization of multi-component transition MC carbides in iron

L. Deillon *, M. Fornabaio, G. Zagar, L. Michelet, A. Mortensen

Ecole Polytechnique Fédérale de Lausanne, CH-1015 Lausanne, Switzerland

ARTICLE INFO

Keywords:
Carbides
Nanoindentation
Hardness
Elastic properties
Tool steel

ABSTRACT

We prepare multi-component transition monocarbides of chosen composition by arc-melting together a pre-alloy of the transition metals and cast iron. Based on the elements Ti, Ta, V, Nb and W, 51 different binary, ternary and quaternary compositions are produced. The intrinsic hardness *H* and modulus *E* of the resulting iron-embedded carbide particles are directly measured using nanoindentation. Of all compositions tested here WC shows the highest modulus while two (Ta,V)C and (Ti,W)C carbides are shown to have a hardness 15% higher than that of all binary carbides; some (Ti,Ta,V)C compositions furthermore display interesting combinations of properties. The modulus and hardness variations with composition show that the valence electron concentration, which has been proposed to be a dominant parameter in predicting carbide hardness and modulus, is not a useful single predictor of optimal compositions. Other important parameters therefore also govern the hardness and modulus of MC carbides.

1. Introduction

1.1. Transition metal carbides

The quest for new super-hard materials, and therefore for reliable hardness predictors, has been running for decades among scientists; see e.g. references [1–3] for a review of different models and some current axes of research. A key for a high hardness seems to lie in the presence, within the material, of an isotropic 3D network of short covalent bonds, consistent with the fact that most cubic monocarbides are very hard.

Transition metal (TM) monocarbides therefore offer a very appealing combination of properties as reinforcing second phases in hard grades of steel since they exhibit high hardness, modulus and melting point values, while being chemically inert in many harsh environments. The fact that transition metals can form very hard compounds with light elements such as carbon or nitrogen has been attributed to a high valence electron density (electrons per unit volume, VED) and a high density of strong and short covalent bonds [4,5] in resulting compounds. While a high bulk modulus is indeed promoted by a high VED [5,6], hardness is, however, a more complex property because the resistance to plastic deformation under a hard indenter cannot be described solely in terms of elastic properties: the phase resistance to plastic flow and to fracture also intervene. In practice, both properties have importance in the performance of materials liable to serve in harsh environments that require a high resistance to both wear and deformation under elevated surface loading.

The ab-initio calculations of Jhi et al. [7] have shown a link between hardness and valence electron concentration (electrons per unit cell, VEC), according to which in some transition metal carbides and carbonitrides (Ti(C,N), Hf(C,N) and (Zr,Nb)C) there should be a maximum in both hardness and shear modulus for a VEC ≈8.4. This trend was already suggested by Holleck [8] based on micro-hardness measurements on different mixed carbides and carbonitrides. Its universal validity can, however, be debated. First, because even if the shear modulus seems to be the elastic property that shows the strongest correlation with hardness [5,9–12] owing to its proportionality to the energy required to nucleate dislocations, the correlation might hide other parameters that intervene in determining the hardness of materials. Secondly, not all data speak eloquently in favour of the VEC being a strong predictor of hardness: in polycrystalline $Ti(C_xN_{1-x})$ samples, with a VEC varying from 8 to 9, no maximum in micro-/nanohardness was observed and measurements of the shear modulus show only a weak maximum at a VEC ≈8.3–8.4 [13,14].

Among the parameters that affect the hardness of binary MC carbides, the carbon content seems to play a major role. For example in TiC, which exhibits a large homogeneity range, the maximum hardness at

* Corresponding author.
E-mail address: lea.deillon@epfl.ch (L. Deillon).

https://doi.org/10.1016/j.jeurceramsoc.2021.02.044
Received 23 December 2020; Received in revised form 23 February 2021; Accepted 24 February 2021
Available online 6 March 2021

$TiC_{0.9}$ (upper limit of homogeneity range) is almost double that of $TiC_{0.5}$ [15]. As for TaC, the maximum H is found with $TaC_{0.8}$, which was roughly twice as hard as stoichiometric TaC [15–17]. Anisotropy, and therefore crystal orientation, is yet another parameter. The hardness of WC [18–27] and that of TiC [28,29] are highly anisotropic. A very wide range of values has been reported for WC; apart from the study of Bonache et al. [27] the hardness measured on the basal plane is always found to be higher than that measured on the prismatic plane, with a strong influence of crystal orientation on the value reported.

A further complication comes from the fact that the production of TM carbides is a challenging task, hindering the collection of experimental data. Samples are most of the time produced by sintering powders, in turn making assessment of their intrinsic mechanical properties subject to the influence of extrinsic parameters such as the presence of pores or grain boundaries. We aim here to complete the sometimes scarce or discrepant literature data on the intrinsic modulus and hardness of binary NbC, TaC, TiC, VC and WC monocarbides via nanoindentation measurements conducted on microscopic dense single crystals of carbide, produced and embedded in an iron matrix by *in-situ* reaction using cast iron as the carbon source, in a way similar to the early technique described by Kieffer and Rassaerts [30]. Of less direct similarity but worthy of mention is the recent work of Cai and Xu [31] who produced NbC films by reaction of Nb with grey cast iron, and that of Wu et al. [32,33] who produced NbC and VC particles by the reaction of a Ni-Cr cast iron with ferroniobium and ferrovanadium, respectively.

Having generated in this way binary or mixed transition monocarbides over a wide composition range we measure their hardness and elastic (indentation) modulus using nanoindentation, searching for optima in those properties. Mixed carbides can indeed show enhanced properties compared to the constitutive binary carbides, as demonstrated by Castle et al. who reported a mixed HfTaZrNbC carbide with a nanoindentation hardness of $H = 36$ GPa and an indentation modulus $M = 598$ GPa (i.e. a Young's modulus $E = 544$–574 GPa assuming a Poisson's ratio $\nu = 0.2$–0.3) [34]. Also in the ternary (Ti,W)C system, Reference [5] in [35] reports a slight maximum in microhardness at 15–20 wt%WC, although no maximum was reported in Reference [161] (original references in Russian).

Mixed TM carbides investigated here are the 5 ternary systems (Nb, Ti)C, (Ta,Ti)C, (Ta,V)C, (Ti,V)C and (Ti,W)C, and several quaternary compositions in the (Ta,Ti,V)C system. Note that, except for (Ti,W)C, all carbide systems investigated here show complete miscibility and, apart for the hexagonal WC phase, all those carbides crystallize with the cubic rock-salt structure.

1.2. Nanoindentation of embedded carbides

Nanoindentation, now a widespread testing method for assessing local micro-mechanical properties [36,37], is particularly suitable for the fast and direct measurement of intrinsic properties of embedded carbide particles of this work; however, one has to be careful with data acquisition, analysis and interpretation. Over the past decades, there have been considerable improvements regarding testing equipment on the one hand, and understanding of the physical phenomena governing indentation on the other hand, leading to improvements in the technique and hence to the acquisition of more accurate and trustworthy results. The Oliver and Pharr [38,39] method is the most common analysis procedure used and has been proven successful for effectively assessing the hardness and elastic modulus of a wide range of materials. One of its major drawbacks lies in the fact that it fails when pile-up or sink-in effects are important, because the contact depth, and hence the contact area, are then misestimated.

When dealing with complex composite microstructures, obtaining meaningful data by indentation is furthermore not straightforward because of the potential influence exerted by other phases present. The testing of hard particles embedded in a softer matrix has thus only scarcely been reported [40,41]. Buchheit and Vogler [40] assessed the hardness and modulus of ceramic particles (ø 25–100 μm) embedded in epoxy via continuous stiffness measurements and corrected their data for an additional, matrix-induced, compliance. Resulting hardnesses were found to be similar to values derived by the classical Oliver and Pharr method, while reduced modulus values were 1 to 8% higher after correction (in most cases within the standard deviation of the measurements). This "structural compliance" correction is similar to the method suggested by Jakes [42], and has also been applied by Takahashi in porous Fe_4N [43].

Table 1
Characteristics of the raw materials.

	Purity [%]	Shape	Supplier
Nb	99.9	Powder	Wah Chang Corporation
Ta	99.98	Powder	abcr GmbH
Ti	99.99	Granules	abcr GmbH
V	99.7	Granules	abcr GmbH
W	99.9	Powder	Alfa Aesar

It is commonly accepted as a rule of thumb that, for an accurate measurement of the intrinsic hardness of a film, the indentation depth should be less than approximately 10% of the film thickness, since at higher indentation depths the substrate starts to yield and the film hardness is underestimated. Bhattacharya and Nix [44] showed by FEM modelling that this holds true for a hard film deposited on a soft substrate. Saha and Nix [45] confirmed this experimentally by obtaining reliable hardness values for a hard W film on a soft Al or glass substrate when the indentation depth was less than approximately 10% of the film thickness. The FEM study of Gamonpilas and Busso [46] also showed that the 10% rule is appropriate when the film-to-substrate yield stress ratio, σ_{yf}/σ_{ys}, is ≥ 10, while if $\sigma_{yf}/\sigma_{ys} > 20$ and the film-to-substrate Young's modulus ratio, E_f/E_s, is >0.1, the indentation depth should remain below 5% of the film thickness (more than 10% if one allows a plastic deformation of 2% in the substrate, which should not result in great error on H). The more recent FEM study of Chen and Bull [47] showed that the hardness of a TiN coating on a steel substrate decreases with increasing relative indentation depth, but does so almost insignificantly below 10% relative indentation depth. This led the authors to conclude that the 10% rule is overall a safe estimate, including for a very hard coating on a softer substrate.

Specific methods have also been developed in order to evaluate the intrinsic elastic properties of thin films when they differ from those of the substrate [45,48–50]. In particular Saha and Nix's [45] modified version of King's model [49] allows for a good estimate of the film modulus when $E_f \lesssim 3E_s$. However the method requires knowledge of the thickness of the film, or particles in our case, and of the elastic properties of the substrate, or matrix in our case. Whereas one can more or less easily measure the (constant) thickness of a deposited film, measurement of the thickness of each embedded particle underneath the load application point would be very tedious, as techniques such as FIB milling would be needed.

In conclusion, given the behaviour of carbides in nanoindentation, given also the relatively high modulus of iron (near one-third that of most carbides), using nanoindentation to measure the hardness and stiffness of carbide particles embedded in steel has the potential to provide reasonably accurate data provided the particles are made to be sufficiently large, by a factor near ten, in comparison to the width and depth of indentations produced during the test.

2. Experimental

Multi-component carbide particles of tailored composition were grown in cast iron according to the following procedure: (i) cast iron was made by induction melting pure iron chips (99.98% purity, Sigma–Aldrich Corporation) in a graphite crucible, (ii) transition metals (characteristics given in Table 1) were pre-alloyed by arc-melting under

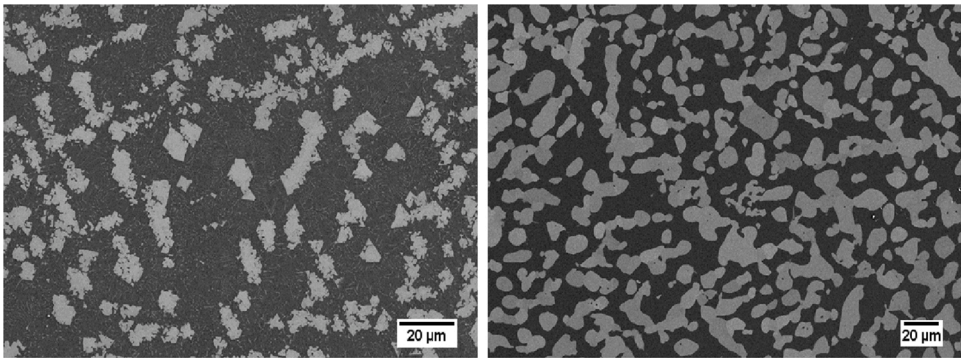

Fig. 1. (Ta,V)C carbide particles after arc-melting (left) and after a heat treatment for 72 h at 1400 °C.

Ar in a laboratory arc melter (Edmund Bühler MAM-1), and (iii) cast iron and the TM pre-alloy were molten together by arc-melting. The resulting samples weighed between 2 to 3 g for a TM carbide content of approximately 40 vol.%. A list of all samples produced and tested in this work is given in the Appendix, Table A.1. In some cases a subsequent heat treatment was carried out to further grow and coarsen the particles and/or homogenize their composition (see e.g. Fig. 1); a detailed list is given in the Appendix, Table A.2.

Samples were then cut, embedded and polished down to 1/4 µm diamond paste for scanning electron microscopy and nanoindentation measurements. SEM imaging was done at 2 kV with a ZEISS Merlin microscope and chemical analyses by energy dispersive X-ray spectroscopy (EDX) with a Oxford Instruments SDD detector at an accelerating voltage of 10 kV. This gives the respective proportions of metallic atoms present within the carbide. Because of the low sensitivity of EDX to carbon, the carbon content and hence potential deviations from metal/carbon atom stoichiometry in the composition of the various carbides analysed here are on the other hand not documented.

Nanoindentation tests were performed with a Hysitron® TI950 TriboIndenter. For hardness measurements a diamond Berkovich indenter was chosen in order to obtain imprints that are deep enough at a moderate load level while limiting the occurrence of cracking. The maximum load P_{max} was set at 6 mN as no load effect was observed on binary carbides in the range 4–10 mN. The tip area function A was calibrated on a fused quartz reference sample and validated on a 4H-SiC wafer (from University Wafer). Data were analysed using the standard Oliver and Pharr method and hence hardness is calculated as:

$$H = \frac{P_{\max}}{A(h_c)} \quad \text{with} \quad h_c = h_{\max} - \varepsilon\frac{P_{\max}}{S} \tag{1}$$

where $\varepsilon = 0.75$ and $S = \frac{dP}{dh}|_{h=h_{\max}}$ is the contact stiffness obtained by fitting the unloading curve (upper 95 to lower 20%) with a power law. The reduced modulus E_r is also calculated from the unloading curve according to:

$$E_r^2 = \frac{\pi}{4}\frac{S^2}{A(h_c)} \tag{2}$$

From those data, the Young's modulus of the tested carbide particles, E, can be derived:

$$\frac{1}{E_r} = \frac{1-\nu_i^2}{E_i} + \frac{1-\nu^2}{E} \tag{3}$$

where ν stands for Poisson's ratio and subscript i refer to the indenter. The Poisson's ratio of ternary and quaternary carbides is calculated by assuming a stoichiometry-based rule of mixtures of values for the relevant binary carbide compositions.

A minimum of 6 particles were tested for each composition, leading to a minimum number of 9 indents for binary carbides (for which there is no change in composition and additional tests with different maximum loads were performed) and 24 for each ternary/quaternary composition. As a check for the correctness of measurements dynamic measurements were also performed on 9 samples (among binary, ternary and quaternary compositions) at a frequency of 165 Hz with a maximum load $P_{max} = 10$ mN.

3. Results

3.1. Microstructural observations

Selected SEM micrographs of carbide particles are presented in Fig. 2. Particles typically show a dendritic morphology after solidification and other phases (Fe-containing carbides and/or intermetallic compounds) are also frequently observed, such as the darker $Fe_2(Ta,V)$ particles present within the $Ta_{90}V_{10}C$ sample (Fig. 2f). The tested particles are typically larger than 10 µm in diameter, the smallest being those of VC with a diameter comprised between 5 and 10 µm. This, in turn, enables nanoindentation testing to be conducted while keeping each nanoindentation below 10% of the carbide particle width or depth.

3.2. Measurement quality checks

Dynamic measurements typically show a plateau in hardness and storage modulus across the load range 4–8 mN, as illustrated in Fig. 3 for a VC particle. Note also that, in this load range, the average hardness values are in agreement with the static measurements presented below, whereas the storage modulus values are found to be 5 to 11% lower than the static values.

Four identical line profiles were drawn across a $Ti_{54}W_{46}C$ particle and the surrounding matrix on scanning probe microscopy (SPM) images recorded before and after 6 indents at 6 mN; scans are shown in Fig. 4. The four line profiles, levelled with respect to the average matrix height, show that the particle height relative to the matrix is the same, within experimental uncertainty, before and after indentation. To quantify this, a numerical integration of the raw (non-smoothed) data curves, before and after indentation, was performed over the distance spanned by the particle, excluding the areas under the indents. The difference between the average particle height relative to the matrix height before and after indentation was found to be less than 1.5 nm, showing that there is no noticeable plastic deformation of the iron matrix induced by the indentations.

3.3. Elastic modulus and hardness

Table 2 summarizes the elastic modulus and hardness measured on particles of the five binary carbides grown within an iron-based matrix. One can see that WC has by far the highest modulus, but also shows more scatter in data than do the other carbides; this is clearly due to its known high level of anisotropy. The modulus of VC is found to be the lowest. In terms of hardness, all values fall in the same range, at around 31 GPa,

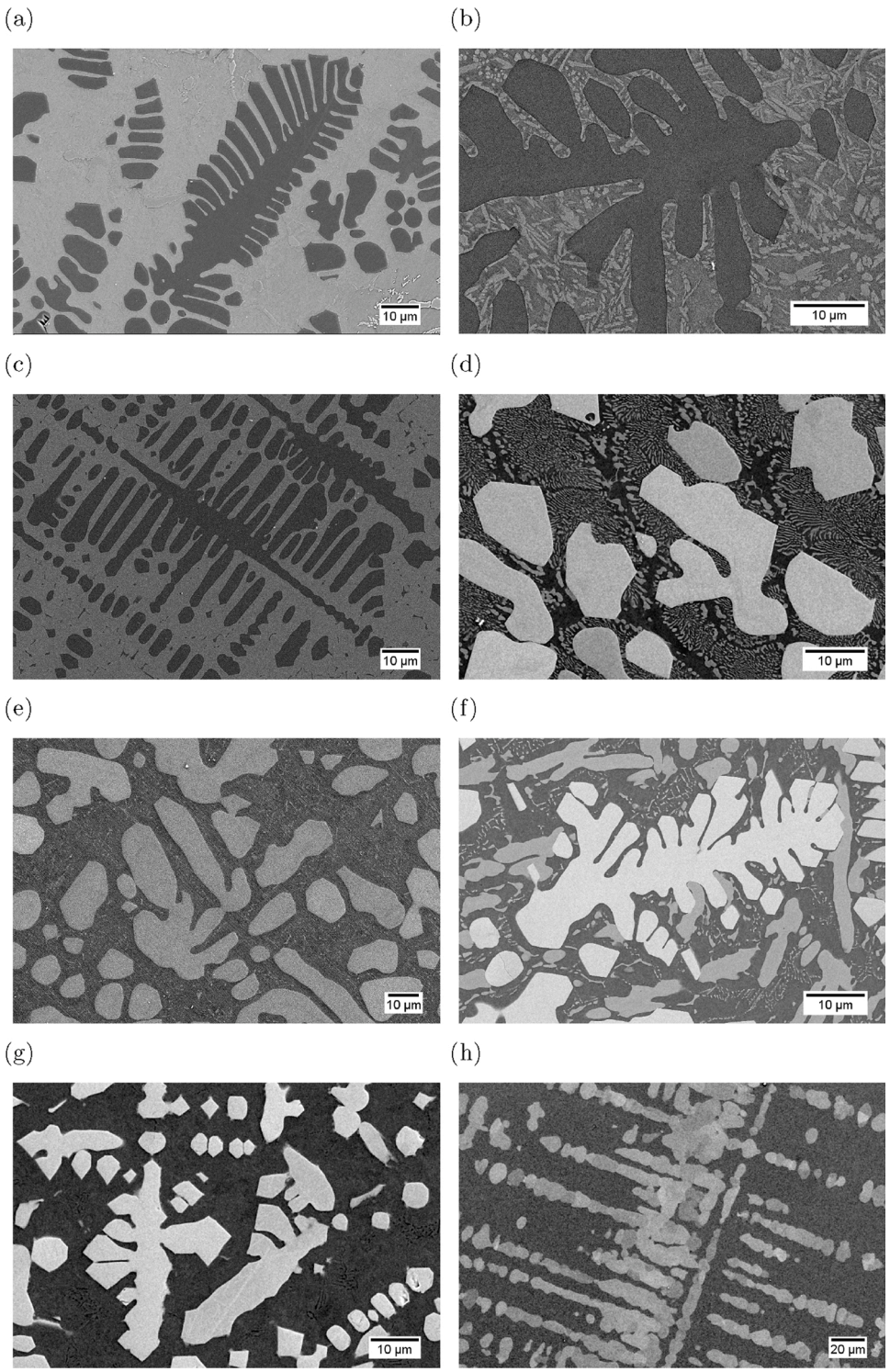

Fig. 2. SEM micrographs of a few carbide particles: (a) TiC, (b) $Ti_{81}W_{19}C$, (c) $Ti_{34}V_{66}C$, (d) $Ti_{22}Ta_{78}C$, (e) $Ti_{23}Nb_{77}C$, (f) $Ta_{90}V_{10}C$, (g) $Ti_{16}Ta_{79}V_3C$ and (h) $Ti_{54}Ta_{22}V_{24}C$ (heat treated 24h at 1400 °C).

except for NbC, the hardness of which is approximately 5 GPa lower.

Results of the hardness and modulus measurements on ternary transition carbide particles are graphically presented in Fig. 5. The error on composition is taken as the larger between (i) the estimated accuracy of the EDX quantifications (±1.5 at.%) and (ii) variations measured within the sample. One can see that no general trend is observed and variations in mechanical properties are highly system-dependent.

In the (Ti,V)C ternary system, carbide particles with a relative Ti content near 50 at.% are found to display the best combination of properties. Indeed hardness data suggest a maximum for *H* of around 33 GPa situated at intermediate compositions, between ~34 and 47 at.% Ti (VEC ≈8.5–8.7), whereas the elastic modulus is highest for Ti-rich compositions. This ternary system is that for which the lowest peak modulus was measured.

The ternary system (Ta,Ti)C shows a different evolution of hardness and modulus with composition. Both properties have a maximum at a relative composition of ~20 at.% Ti (VEC ≈8.8), while a minimum is observed for a VEC ≈8.3. The maximum hardness is again about 33 GPa,

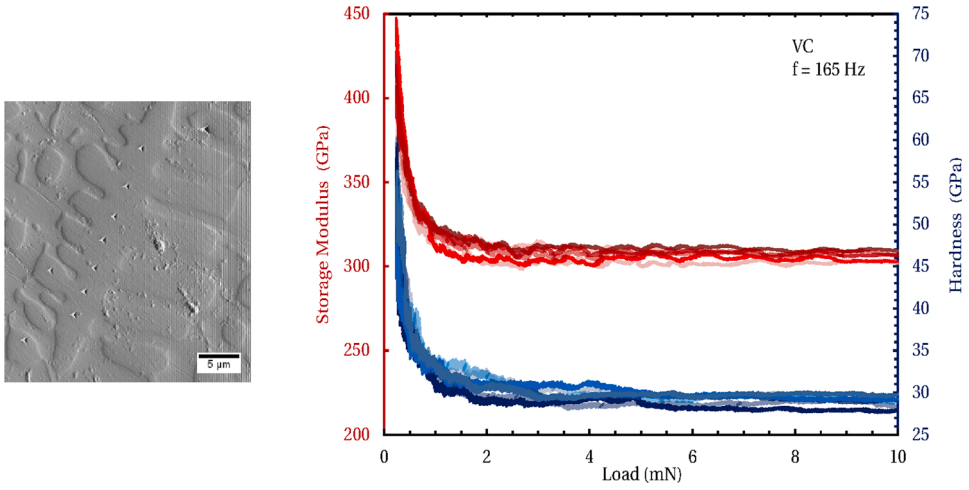

Fig. 3. Hardness and modulus of a VC particle from dynamic measurements. Top right and bottom left indents were discarded because of their proximity to the matrix.

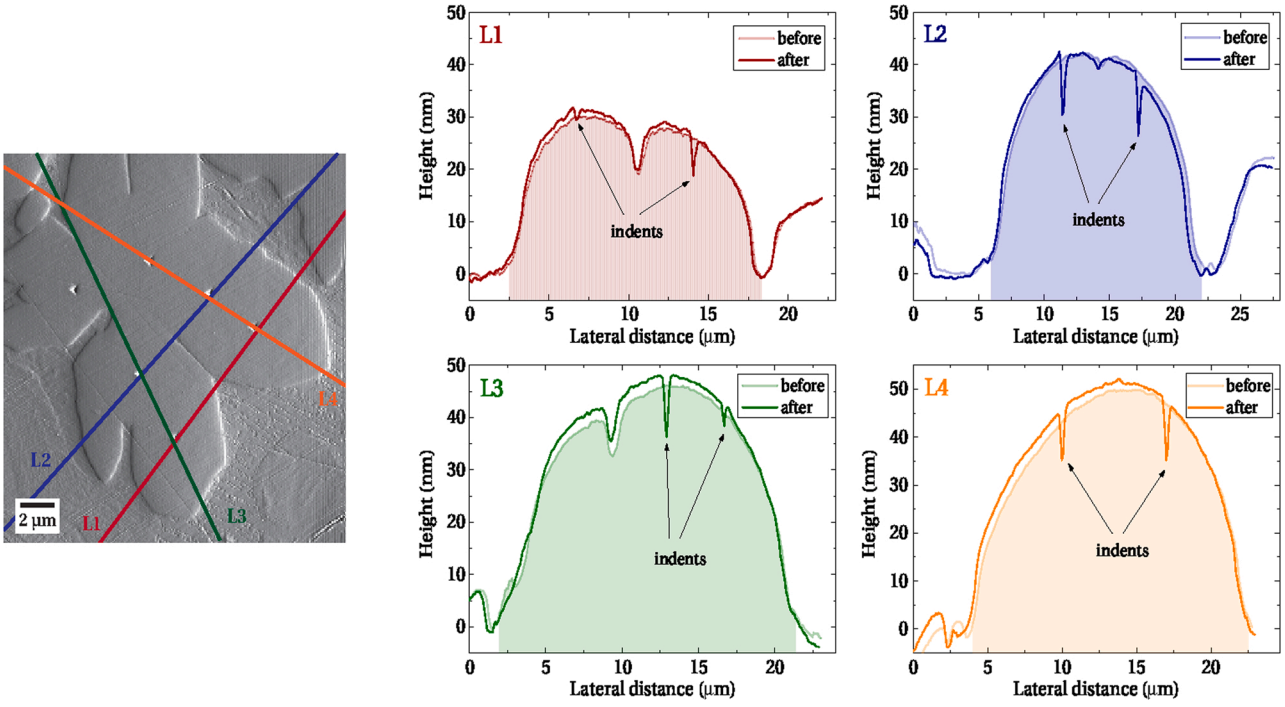

Fig. 4. Scanning probe microscopy (SPM) image and line profiles before and after 6 indents in a $Ti_{54}W_{46}C$ particle.

Table 2
Elastic modulus and hardness of binary carbide particles; values of Poisson's ratio used in the calculation of E are also reported. The error values correspond to the standard deviation of the measurements.

	E [GPa]	H [GPa]	ν [–]
NbC	455 ± 14	25.7 ± 1.2	0.22 [51–53]
TaC	487 ± 14	31.6 ± 0.8	0.24 [51,54]
TiC	473 ± 6	30.9 ± 0.7	0.20 [53,55]
VC	418 ± 8	30.4 ± 0.9	0.22 [52,53]
WC	637 ± 32	31.1 ± 3.4	0.24 [56,57]

but compared to the (Ti,V)C system higher moduli are found.

The VEC is constant in the (Ta,V)C system, since both Ta and V belong to Group V of the periodic table. Ta-rich compositions of mixed (Ta,V)C carbides display the highest values of hardness and modulus, both being found at a relative composition of ~90 at.% Ta. Hardness reaches here a maximum of 36±1 GPa and hence exceeds the values found in the two preceding ternary systems. Note, however, that two very close compositions show significant differences, one having a considerably higher hardness but a lower modulus than the other.

Within uncertainty, the hardness of (Nb,Ti)C carbides does not show significant variation, with all values lying in the range 30–33 GPa except for binary NbC. Hence in this system a small addition of Ti is already sufficient to bring the hardness of the carbide to a level comparable to that of binary TiC. On the other hand, a maximum in elastic modulus is found at a Ti relative content of approximately 20 at.% (VEC ≈8.8), which makes this composition the most interesting within this system in terms of H and E combined.

In the (Ti,W)C ternary system, peak hardness is found at ~40 at.% Ti, while no intermediate composition is able to compete with the high modulus of binary WC. The peak H value at 36.4 ± 1.5 GPa represents

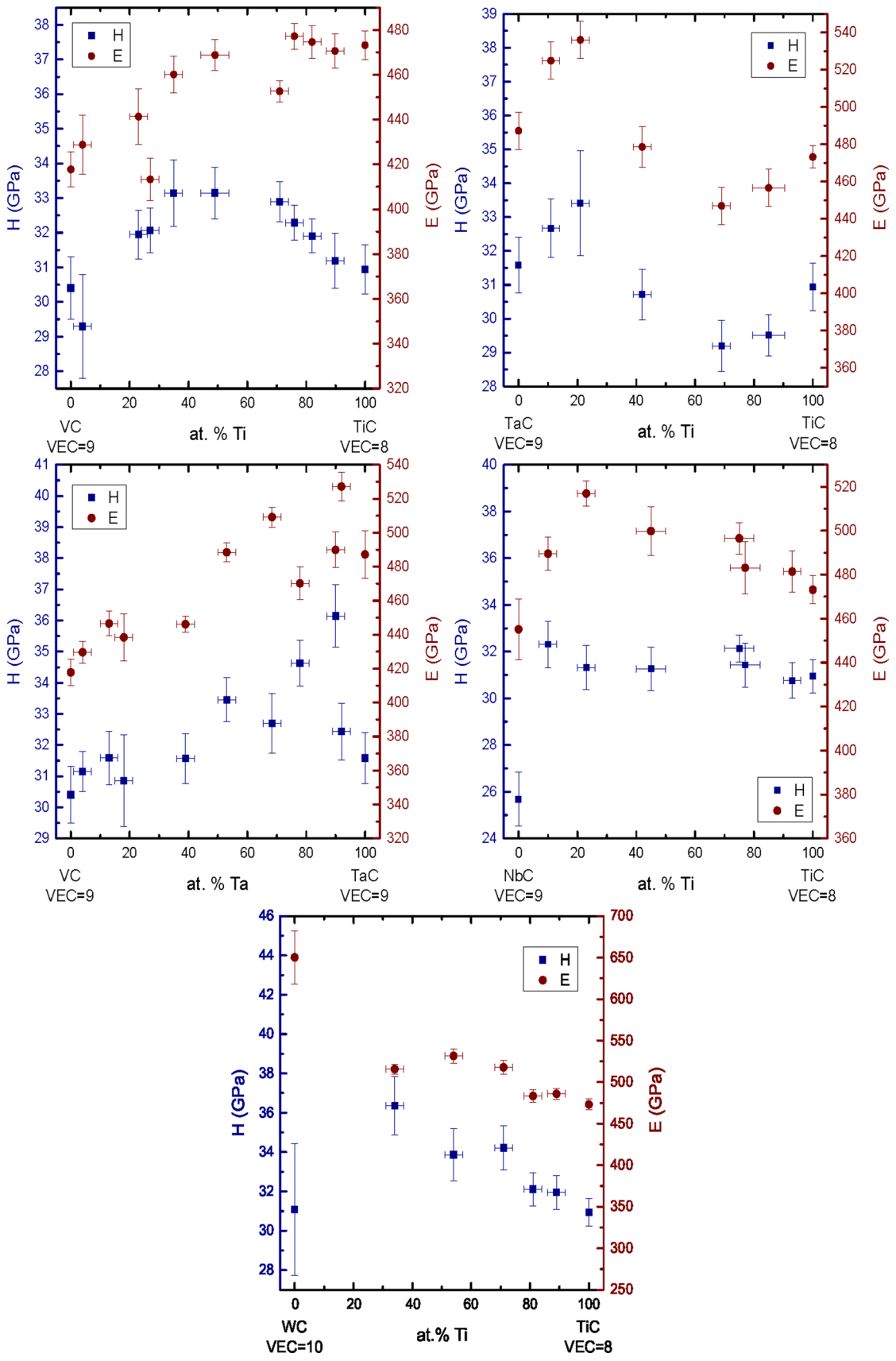

Fig. 5. Evolution of the hardness and elastic modulus in the (Ti,V)C, (Ta,Ti)C, (Ta,V)C, (Nb,Ti)C and (Ti,W)C systems.

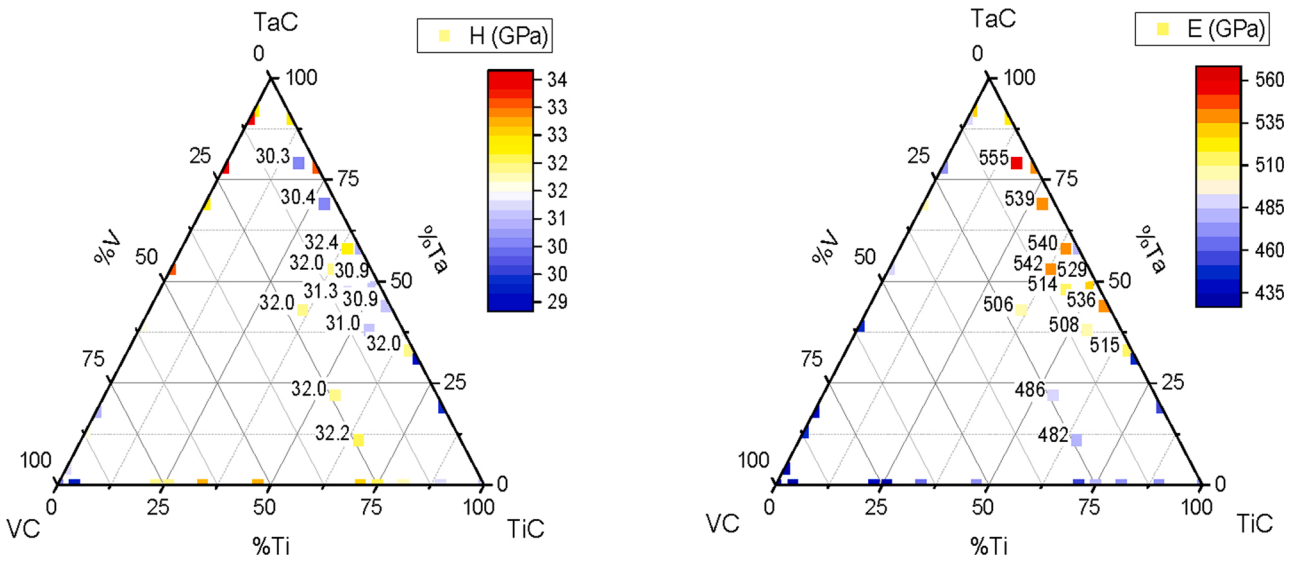

Fig. 6. Ternary diagrams showing the hardness (left) and modulus (right) of quaternary (Ti,Ta,V)C carbides.

Table 3
Hardness of binary carbides: present measurements and comparison with literature data.

	H [GPa]	H_{lit} [GPa]
NbC	25.7 ± 1.2	25.5–33.8 [32,58]
TaC	31.6 ± 0.8	18–29 [34,59,60]
TiC	30.9 ± 0.7	~32 [14]
VC	30.4 ± 0.9	~35 [58]
WC	31.1 ± 3.4	17–55 [21–27,40]

the highest value of hardness that we measured in this work.

Results of the hardness and elastic modulus measurements on quaternary transition carbides are graphically presented in Fig. 6. All hardness values are found to lie within the range 30.3–32.4 GPa, i.e. in the same ballpark as the hardnesses of the 3 constituent binary carbides. Higher values of modulus, comprised between 540 and 555 GPa, are on the other hand observed for carbides containing a low amount of V and more Ta than Ti. These values represent a 10–15% increase as compared to binary TaC or TiC.

4. Discussion

We begin with a few general observations before discussing modulus and hardness values that we measured; those are collated in the appendix, Table A.1. First, across samples tested here we did not observe a correlation between hardness and particle size. Secondly, residual stresses are present within the carbide particles due to the mismatch in coefficient of thermal expansion between the carbide particles and the iron matrix, coupled with the significant temperature excursion between the iron phase solidification temperature (or heat treatment temperature if relevant) and room temperature. Working numbers leads to conclude that (compressive) residual stress values in the carbide particles are at most on the order of a few GPa, i.e. an order of magnitude lower than measured carbide hardness values, and likely much lower owing to matrix plastic deformation and the fact that particles were tested along a free surface. Residual stresses are thus unlikely to have significantly influenced nanoindentation data of this work. This is corroborated by the fact that the hardness of samples that were subjected to a subsequent thermal treatment is not systematically lower than values measured in samples that were rapidly solidified and brought to room temperature in the arc-melter.

4.1. Binary carbides

Given the large range of reported values and/or the scarcity of data in the literature, present values for the hardness of binary MC carbides are overall consistent with previous published results, see Table 3. The results for TiC, WC and NbC are in agreement with previous studies, whereas our value for TaC is slightly higher, and that for VC lower, than what is reported in the literature. We observe a relatively small dispersion of our values for TiC, despite the anisotropy of hardness observed by Maerky et al. [28] and Kumashiro et al. [29].

The relatively high hardness of TaC particles, compared to literature data gleaned on sintered powders, might be due to a carbon deficiency when those carbides are grown from the melt. Impurities may also play a role since in [59] and [34] the authors found $H = 18$–22 GPa using a TaC powder of 99.5% purity from the same supplier, H.C. Stark, while in [60] the authors found $H = 26 \pm 3$ GPa with a powder of 99.7% purity from Inframat Advanced Materials LLC. Note also that most published hardness values obtained via nanoindentation have been measured on samples made of sintered powders that contained some amount of porosity [14,34,58,59], and sometimes on particles that were insufficiently large (~1 μm) compared to the size of the indents [22,25–27].

Anisotropy, as mentioned in the introduction, constitutes a potential source of discrepancy. We note, however, that the magnitude of the standard deviations on the hardness and elastic modulus values of all cubic carbides tested here is rather small, suggesting, either that tested particles were not randomly oriented, or if randomly oriented particles were tested, that those are only weakly anisotropic.

One could have expected a correlation between group and hardness since Group IV (TiC, ZrC, HfC) transition metal carbides have fewer metallic bonds than Group V (TaC, NbC, VC) or Group VI carbides. Furthermore in Group IV monocarbides slip is predominant in the {110} planes whereas slip in Group V monocarbides mostly takes place in {111} slip planes [61,62]. DFT calculations of De Leon et al. [62] showed that {110} slip is energetically favourable in all of the transition carbides, but also revealed the presence of an intrinsic stacking fault (ISF) in the {111} plane of Group V carbides. Calculations of dislocation energies using a Peierls Nabarro model showed that this ISF makes it energetically favourable for dislocations in the {111} plane to decompose into Shockley partials, which lowers the energy barrier for the motion of {111} dislocations in Group V carbides. In our measurements NbC is the only binary carbide (from Group V) with a hardness lower than that of TiC, and hence our results do not provide confirmation of a correlation between metal group and hardness.

Table 4
Elastic modulus of binary carbides: present measurements compared with experimental literature data.

	E [GPa]	E_{lit} [GPa]
NbC	455 ± 14	488–550 [51,63]
TaC	487 ± 14	537–567 [51,54,64–66]
TiC	473 ± 6	436–467 [63,65,67–70]
VC	418 ± 8	430 [63]
WC	637 ± 32	623–722 [51,56,63,71]

For the elastic modulus only data obtained via ultrasonic measurements on single crystals or sintered powder extrapolated to full density are considered here as trustworthy literature experimental data. One can see that our data compare fairly well with the literature (Table 4), except again for TaC particles whose modulus is lower than the range of previously reported values. Note that values from density functional theory (DFT) calculations, when available, have such a large spread that they yield an overly vague comparison with the measurements we report here (419–611 GPa for NbC [32,52,53,72–76], 492–680 GPa for TaC [32,53,74,75] and 401–481 GPa for TiC [53,55,72–77].

4.2. Properties of ternary and quaternary carbides

The discrepancy in hardness and modulus observed between the two (Ta,V)C samples containing carbides of composition near 90% Ta remains unexplained since the two samples were processed identically and contain the same impurity levels. There is yet a difference in microstructure between these two samples: the harder sample contains carbides of more dendritic character and the carbide particles are also of size and shape such that the two samples having been cut along differently oriented planes of the same (anisotropic) microstructure can be excluded. Hence there might have been a difference in the cooling rate at which each of the two samples was solidified which might, in turn, have resulted in carbides with different carbon content. A difference in carbon stoichiometry is however difficult to measure.

The maximum solubility of W in the cubic TiC structure is about 50 at.% at 1500 °C and decreases with temperature [78,79]. This means that the two compositions $Ti_{34}W_{66}C$ and $Ti_{54}W_{46}C$, which show the highest hardness values in this system and values of modulus that are among the highest that we measured, are actually metastable compositions.

For ternary systems exhibiting complete miscibility it is possible to compare the change in mechanical properties with the change in lattice parameter a (values for cubic binary carbides are given in the Appendix, Table A.3). The magnitude of change in a is the highest in the (Ta,V)C system ($\Delta a = 6.5\%$), which also shows the largest variation in E (~100 GPa) and the second largest variation in H. This being noted, the agreement stops here since (i) most of the ternary systems do not show a linear or even regular evolution in mechanical properties with composition whereas it seems reasonable to assume that a does according to Vegard's law, (ii) the second largest variation in E (~90 GPa) is observed in the (Ta,Ti)C system which has also the smallest variation in a (3%), and (iii) the largest variation in H (~6 GPa) is observed in (Nb,Ti)C carbides, i.e. in the second to last system in terms of the extent of variation in a (3.5%).

Although the (Ta,V)C system has a constant VEC, it shows significant variations in both Young's modulus and hardness. This implies that VEC alone is not a satisfactory criterion to predict hardness or modulus maxima; systematic prediction of the hardness and stiffness of MC carbides seemingly requires accounting for the effect of additional parameters such as a potential solid solution hardening caused by different atomic radii or a change in vacancy concentration. Some work along this direction can already be found in the literature. For example, Gao [80] proposed a model to estimate the (Knoop) hardness of cubic solid solutions which, in addition to atomic bonding characteristics, takes into account various other parameters such as the orientation of the indenter with respect to the glide planes, the atomic size misfit, the fraction of solute atoms, and to some extent the brittleness. This model is able to reproduce some experimental trends but still shows some deviations for the transition metal carbides (Nb,Ti)C and (Nb,Zr)C, which Gao attributes to the complex mixed nature of their atomic bonds. Therefore, key parameters governing the hardness of carbides remain to be fully unravelled. In particular it seems essential to assess whether a high hardness arises from barriers opposing dislocation nucleation or dislocation propagation. Ab-initio prediction of maxima in elastic modulus seems more within reach nowadays, although from the large range of calculated values found for binary carbides it is clear that current methods still need refinement.

5. Conclusion

Multi-component transition metal carbide particles of tailored composition and suitable for testing can be produced by arc-melting together cast iron and a pre-alloy of the transition metals.

The standard Oliver and Pharr method was used to assess the intrinsic hardness and modulus of iron-embedded carbide particles from indentation curves at a maximum load of 6 mN since (i) dynamic measurements show a plateau in hardness and storage modulus in the load range 4–8 mN, (ii) present carbide particles are thicker than 5 µm and therefore well above 10× the indentation depth (~100 nm at 6 mN), (iii) pre and post SPM scans show an absence of matrix plastic deformation and no significant pile-up or sink-in effects, and (iv) indentation curves within a single particle superimpose well.

Hardness values for binary carbide particles grown within a Fe matrix are overall consistent with (scarce and highly variable) values in the literature. Hardness maxima are found for the ternary carbides $Ti_{34}W_{66}C$ (36.4 ± 1.5 GPa) and $Ta_{90}V_{10}C$ (36.1 ± 1.0 GPa); these values represent a 15% increase compared to those of the binary carbides. It is also noteworthy that substituting 50% W with Ti in WC leads to an equally performant carbide while using a less scarce element to produce it.

Measured maxima in hardness are not located at a VEC ≈8.4; furthermore, the (Ta,V)C system with a constant VEC also shows variations in hardness. The VEC alone thus fails to predict optimum compositions, leading to conclude that others parameters intervene.

Concerning the elastic modulus of MC carbides, values for TaC and NbC particles of this work are lower than the previously reported values for those binary carbides. We found no ternary/quaternary carbide that is able to compete with WC in terms of modulus. Among other carbides explored here the highest E are found for quaternary (Ti,Ta,V)C compositions with a low V and a high Ta content. Variations in modulus are also not found to be correlated with the VEC.

Conflict of interest

The authors declare no conflict of interest.

Declaration of Competing Interest

The authors report no declarations of interest.

Acknowledgement

This research was funded by the European Research Council under the European Union's Seventh Framework Programme (FP/2007–2013)/ERC Advanced Grant Agreement No. 291085. We note that data reported here differ from, and supersede, (unpublished) data in the original version of the PhD thesis of Lionel Michelet (which were shown at the 55th Annual Technical meeting Society of Engineering Science, October 10–12, 2018, in Madrid, Spain), as those data have unfortunately been found, after the thesis was defended, to contain errors.

Appendix A

Table A.1
Composition and mechanical properties of all tested carbides.

Composition [at.%]	E [GPa]	H [GPa]
NbC	455 ± 14	25.7 ± 1.2
TaC	487 ± 14	31.6 ± 2
TiC	473 ± 6	30.9 ± 0.7
VC	418 ± 8	30.4 ± 0.9
WC*	637 ± 32	31.1 ± 3.4
$Ta_{92}V_8C$	527 ± 8	32.4 ± 0.9
$Ta_{90}V_{10}C$	490 ± 10	36.1 ± 1.0
$Ta_{78}V_{22}C$[a]	470 ± 10	34.6 ± 0.7
$Ta_{68}V_{32}C$[a]	509 ± 6	32.7 ± 1.0
$Ta_{53}V_{47}C$[a]	488 ± 6	33.5 ± 0.7
$Ta_{39}V_{61}C$[a]	446 ± 5	31.6 ± 0.8
$Ta_{18}V_{82}C$[a]	438 ± 14	30.9 ± 1.5
$Ta_{13}V_{87}C$[a]	447 ± 7	31.6 ± 0.9
$Ta_4V_{96}C$	430 ± 6	31.2 ± 0.6
$Ti_{10}Nb_{90}C$	490 ± 8	32.3 ± 1.0
$Ti_{23}Nb_{77}C$	517 ± 6	31.3 ± 0.9
$Ti_{45}Nb_{55}C$[a]	500 ± 11	31.3 ± 0.9
$Ti_{75}Nb_{25}C$[a]	497 ± 7	32.1 ± 0.6
$Ti_{77}Nb_{23}C$[a]	485 ± 7	31.9 ± 0.9
$Ti_{93}Nb_7C$	481 ± 9	30.8 ± 0.8
$Ti_{11}Ta_{89}C$	525 ± 7	32.7 ± 0.9
$Ti_{21}Ta_{79}C$	536 ± 5	33.4 ± 1.5
$Ti_{42}Ta_{58}C$	479 ± 9	30.7 ± 0.7
$Ti_{69}Ta_{31}C$	447 ± 11	29.2 ± 0.8
$Ti_{85}Ta_{15}C$	457 ± 6	29.5 ± 0.6
$Ti_{90}V_{10}C$	471 ± 8	31.2 ± 0.8
$Ti_{82}V_{18}C$	475 ± 7	31.9 ± 0.5
$Ti_{76}V_{24}C$	477 ± 6	32.3 ± 0.5
$Ti_{71}V_{29}C$	453 ± 5	32.9 ± 0.6
$Ti_{49}V_{51}C$	469 ± 7	33.1 ± 0.7
$Ti_{35}V_{65}C$	460 ± 8	33.1 ± 1.0
$Ti_{27}V_{73}C$	413 ± 9	32.1 ± 0.7
$Ti_{23}V_{77}C$	441 ± 12	31.9 ± 0.7
$Ti_4V_{96}C$	429 ± 13	29.3 ± 1.5
$Ti_{34}W_{66}C$	516 ± 6	36.4 ± 1.5
$Ti_{54}W_{46}C$	532 ± 9	33.9 ± 1.3
$Ti_{71}W_{29}C$	518 ± 8	34.2 ± 1.1
$Ti_{81}W_{19}C$	483 ± 8	32.1 ± 0.8
$Ti_{89}W_{11}C$	486 ± 7	31.9 ± 0.9
$Ti_{66}Ta_{33}V_1C$	515 ± 9	32.0 ± 0.6
$Ti_{55}Ta_{44}V_1C$	536 ± 8	30.9 ± 1.0
$Ti_{49}Ta_{49}V_2C$	529 ± 9	30.9 ± 1.1
$Ti_{39}Ta_{58}V_3C$	540 ± 8	32.4 ± 0.9
$Ti_{28}Ta_{69}V_3C$	539 ± 9	30.4 ± 0.9
$Ti_{17}Ta_{79}V_4C$	555 ± 7	30.3 ± 1.2
$Ti_{54}Ta_{38}V_8C$	508 ± 10	31.0 ± 0.9
$Ti_{44}Ta_{48}V_8C$	514 ± 7	31.3 ± 1.0
$Ti_{38}Ta_{53}V_9C$[a]	542 ± 7	32.0 ± 1.1
$Ti_{65}Ta_{11}V_{24}C$[a]	482 ± 7	32.2 ± 1.2
$Ti_{54}Ta_{22}V_{24}C$[a]	486 ± 7	32.0 ± 1.1
$Ti_{36}Ta_{43}V_{21}C$[a]	506 ± 6	32.0 ± 1.2

[a] Heat-treated samples, see Table A.2.

Table A.2
List of samples subjected to heat treatment and conditions thereof.

Composition	T [°C]	t [h]
WC	1400	2
$Ti_{77}Nb_{23}C$	1250	72
$Ti_{75}Nb_{25}C$	1350	1
$Ti_{45}Nb_{55}C$	1200	48
$Ta_{78}V_{22}C$	1400	72
$Ta_{68}V_{32}C$	1400	2
$Ta_{53}V_{47}C$	1400	2
$Ta_{39}V_{61}C$	1400	2
$Ta_{18}V_{82}C$	1400	72
$Ta_{13}V_{87}C$	1350	2
$Ti_{38}Ta_{53}V_9C$	1500	2
$Ti_{65}Ta_{11}V_{24}C$	1400	24
$Ti_{54}Ta_{22}V_{24}C$	1400	24
$Ti_{36}Ta_{43}V_{21}C$	1400	24

Table A.3
Lattice parameter of cubic binary carbides [81].

	a [Å]
NbC	4.454
TaC	4.453
TiC	4.325
VC	4.163

References

[1] Y. Tian, B. Xu, Z. Zhao, Microscopic theory of hardness and design of novel superhard crystals, Int. J. Refract. Metals Hard Mater. 33 (2012) 93–106.
[2] P. Sarker, T. Harrington, C. Toher, C. Oses, M. Samiee, J.P. Maria, D.W. Brenner, K. S. Vecchio, S. Curtarolo, High-entropy high-hardness metal carbides discovered by entropy descriptors, Nat. Commun. 9 (2018) 1–10.
[3] T.J. Harrington, J. Gild, P. Sarker, C. Toher, C.M. Rost, O.F. Dippo, C. McElfresh, K. Kaufmann, E. Marin, L. Borowski, P.E. Hopkins, J. Luo, S. Curtarolo, D. W. Brenner, K.S. Vecchio, Phase stability and mechanical properties of novel high entropy transition metal carbides, Acta Mater. 166 (2019) 271–280.
[4] R.B. Kaner, J.J. Gilman, S.H. Tolbert, Materials science: designing superhard materials, Science (80-) 308 (2005) 1268–1269.
[5] J.J. Gilman, R.W. Cumberland, R.B. Kaner, Design of hard crystals, Int. J. Refract. Metals Hard Mater. 24 (2006) 1–5.
[6] C. Li, P. Wu, Correlation of bulk modulus and the constituent element properties of binary intermetallic compounds, Chem. Mater. 13 (2001) 4642–4648.
[7] S.-H. Jhi, J. Ihm, S.G. Louie, M.L. Cohen, Electronic mechanism of hardness enhancement in transition-metal carbonitrides, Nature 399 (1999) 132–134.
[8] H. Holleck, Material selection for hard coatings, J. Vac. Sci. Technol. A Vac. Surf. Film 4 (1986) 2661–2669.
[9] D.M. Teter, Computational alchemy: the search for new superhard materials, MRS Bull. 23 (1998) 22–27.
[10] J.M. Léger, P. Djemia, F. Ganot, J. Haines, A.S. Pereira, J.A. Da Jornada, Hardness and elasticity in cubic ruthenium dioxide, Appl. Phys. Lett. 79 (2001) 2169–2171.
[11] V.V. Brazhkin, A.G. Lyapin, R.J. Hemley, Harder than diamond: dreams and reality, Philos. Mag. A Phys. Condens. Matter. Struct. Defects Mech. Prop. 82 (2002) 231–253.
[12] J. Haines, J. Léger, G. Bocquillon, Synthesis and design of superhard materials, Annu. Rev. Mater. Res. 31 (2001) 1–23.
[13] W. Lengauer, S. Binder, K. Aigner, P. Ettmayer, A. Guillou, J. Debuigne, G. Groboth, Solid state properties of group IVb carbonitrides, J. Alloys Compd. 217 (1995) 137–147.
[14] Q. Yang, W. Lengauer, T. Koch, M. Scheerer, I. Smid, Hardness and elastic properties of Ti(CxN1-x), Zr(CxN1-x) and Hf(CxN1-x), J. Alloys Compd. 309 (2000) 5–9.
[15] H.E. Exner, Physical and chemical nature of cemented carbides, Int. Metals Rev. 24 (1979) 149–170.
[16] G. Santoro, Variation of some properties of tantalum carbide with carbon content, Trans. Metall. Soc. AIME 227 (1963) 1361–1368.
[17] D.J. Rowcliffe, W.J. Warren, Structure and properties of tantalum carbide crystals, J. Mater. Sci. 5 (1970) 345–350.
[18] T. Takahashi, E.J. Freise, Determination of the slip systems in single crystals of tungsten monocarbide, Philos. Mag. 12 (1965) 1–8.
[19] D.N. French, D.A. Thomas, Hardness anisotropy and slip in WC crystals, Trans. Metall. Soc. AIME 233 (1965) 950–952.
[20] M. Malli, E. Hillnhagen, Metallographic investigations on WC single crystals, Pract. Metallogr. 4 (1967) 16–27.
[21] J.J. Roa, E. Jimenez-Pique, C. Verge, J.M. Tarragó, A. Mateo, J. Fair, L. Llanes, Intrinsic hardness of constitutive phases in WC-Co composites: nanoindentation testing, statistical analysis, WC crystal orientation effects and flow stress for the constrained metallic binder, J. Eur. Ceram. Soc. 35 (2015) 3419–3425.
[22] J.J. Roa, P. Sudharshan Phani, W.C. Oliver, L. Llanes, Mapping of mechanical properties at microstructural length scale in WC-Co cemented carbides: assessment of hardness and elastic modulus by means of high speed massive nanoindentation and statistical analysis, Int. J. Refract. Metals Hard Mater. 75 (2018) 211–217.
[23] T. Csanádi, M. Bl'Anda, N.Q. Chinh, P. Hvizdoš, J. Dusza, Orientation-dependent hardness and nanoindentation-induced deformation mechanisms of WC crystals, Acta Mater. 83 (2015) 397–407.
[24] N. Cuadrado, D. Casellas Padró, L.M. Llanes Pitarch, I. Gonzalez, J. Caro, Effect of crystal anisotropy on the mechanical properties of WC embedded in WC-Co cemented carbides, Proc. Euro PM2011 Powder Metall. Congr. Exhib. (2011) 215–220.
[25] A. Duszová, R. Halgaš, M. Blanda, P. Hvizdoš, F. Lofaj, J. Dusza, J. Morgiel, Nanoindentation of WC-Co hardmetals, J. Eur. Ceram. Soc. 33 (2013) 2227–2232.
[26] M. Blanda, A. Duszová, T. Csanádi, P. Hvizdoš, F. Lofaj, J. Dusza, Indentation hardness and fatigue of WC – Co composites, Int. J. Refract. Metals Hard Mater. 49 (2015) 178–183.
[27] V. Bonache, E. Rayón, M. Salvador, D. Busquets, Nanoindentation study of WC-12Co hardmetals obtained from nanocrystalline powders: evaluation of hardness and modulus on individual phases, Mater. Sci. Eng. A 527 (2010) 2935–2941.
[28] C. Maerky, M.-O. Guillou, J.L. Henshall, R.M. Hooper, Indentation hardness and fracture toughness in single crystal TiC, Mater. Sci. Eng. A 209 (1996) 329–336.

[29] Y. Kumashiro, A. Itoh, T. Kinoshita, M. Sobajima, The micro-vickers hardness of TIC single crystals at high temperature, Bull. Electrotech. Lab. 41 (1977) 600–609.
[30] R. Kieffer, H. Rassaerts, The use of an auxiliary metal bath for the production of high purity carbide powders of the IVa-VIa Group of Elements, Int. J. Powder Metall. 2 (1966) 15–22.
[31] X. Cai, Y. Xu, Microstructure, friction and wear of NbC coatings on a Fe substrate fabricated via an in situ reaction, Surf. Coat. Technol. 322 (2017) 202–210.
[32] L. Wu, Y. Wang, Z. Yan, J. Zhang, F. Xiao, B. Liao, The phase stability and mechanical properties of Nb – C system: using first-principles calculations and nano-indentation, J. Alloys Compd. 561 (2013) 220–227.
[33] L. Wu, T. Yao, Y. Wang, J. Zhang, F. Xiao, B. Liao, Understanding the mechanical properties of vanadium carbides: nano-indentation measurement and first-principles calculations, J. Alloys Compd. 548 (2013) 60–64.
[34] E. Castle, T. Csanádi, S. Grasso, J. Dusza, M. Reece, Processing and properties of high-entropy ultra-high temperature carbides, Sci. Rep. 8 (2018) 8609.
[35] G.S. Kreimer, Strength of hard alloys, Consultants Bureau, New York, 1968.
[36] G.M. Pharr, Y.T. Cheng, I.M. Hutchings, M. Sakai, N.R. Moody, G. Sundararajan, M. V. Swain, Introduction, J. Mater. Res. 24 (2009) 579–580.
[37] A.C. Fischer-Cripps, Nanoindentation, Mechanical Engineering Series, 3rd edition, Springer New York, New York, NY, 2011.
[38] G.M. Pharr, W.C. Oliver, Measurement of thin film mechanical properties using nanoindentation, MRS Bull. 17 (1992) 28–33.
[39] W. Oliver, G. Pharr, Measurement of hardness and elastic modulus by instrumented indentation: advances in understanding and refinements to methodology, J. Mater. Res. (2004).
[40] T.E. Buchheit, T.J. Vogler, Measurement of ceramic powders using instrumented indentation and correlation with their dynamic response, Mech. Mater. 42 (2010) 599–614.
[41] H.Y. Amanieu, D. Rosato, M. Sebastiani, F. Massimi, D.C. Lupascu, Mechanical property measurements of heterogeneous materials by selective nanoindentation: application to LiMn2O4 cathode, Mater. Sci. Eng. A 593 (2014) 92–102.
[42] J. Jakes, C. Frihart, J. Beecher, R. Moon, D. Stone, Experimental method to account for structural compliance in nanoindentation measurements, J. Mater. Res. 23 (2008) 1113–1127.
[43] T. Takahashi, J. Burghaus, D. Music, R. Dronskowski, J.M. Schneider, Elastic properties of γ'-Fe 4N probed by nanoindentation and ab initio calculation, Acta Mater. 60 (2012) 2054–2060.
[44] A.K. Bhattacharya, W.D. Nix, Analysis of elastic and plastic deformation associated with indentation testing of thin films on substrates, Int. J. Solids Struct. 24 (1988) 1287–1298.
[45] R. Saha, W.D. Nix, Effects of the substrate on the determination of thin film mechanical properties by nanoindentation, Acta Mater. 50 (2002) 23–38.
[46] C. Gamonpilas, E.P. Busso, On the effect of substrate properties on the indentation behaviour of coated systems, Mater. Sci. Eng. A 380 (2004) 52–61.
[47] J. Chen, S.J. Bull, On the factors affecting the critical indenter penetration for measurement of coating hardness, Vacuum 83 (2009) 911–920.
[48] M.F. Doerner, D.S. Gardner, W.D. Nix, Plastic properties of thin films on substrates as measured by submicron indentation hardness and substrate curvature techniques, J. Mater. Res. 1 (1986) 845–851.
[49] R.B. King, Elastic analysis of some punch problems for a layered medium, Int. J. Solids Struct. 23 (1987) 1657–1664.
[50] J. Hay, B. Crawford, Measuring substrate-independent modulus of thin films, J. Mater. Res. 26 (2011) 727–738.
[51] H.L. Brown, P.E. Armstrong, C.P. Kempter, Elastic properties of some polycrystalline transition-metal monocarbides, J. Chem. Phys. 45 (1966) 547–549.
[52] P. Soni, G. Pagare, S.P. Sanyal, Structural, high pressure and elastic properties of transition metal monocarbides: a FP-LAPW study, J. Phys. Chem. Solids 72 (2011) 810–816.
[53] G. Sai Gautam, K.C. Hari Kumar, Elastic, thermochemical and thermophysical properties of rock salt-type transition metal carbides and nitrides: a first principles study, J. Alloys Compd. 587 (2014) 380–386.
[54] L. López-de-la Torre, B. Winkler, J. Schreuer, K. Knorr, M. Avalos-Borja, Elastic properties of tantalum carbide (TaC), Solid State Commun. 134 (2005) 245–250.
[55] Y. Yang, H. Lu, C. Yu, J.M. Chen, First-principles calculations of mechanical properties of TiC and TiN, J. Alloys Compd. 485 (2009) 542–547.
[56] M. Lee, R. Gilmore, Single crystal elastic constants of tungsten monocarbide, J. Mater. Sci. 17 (1982) 2657–2660.
[57] T. Csanádi, M. Blanda, A. Duszová, N.Q. Chinh, P. Szommer, J. Dusza, Deformation characteristics of WC micropillars, J. Eur. Ceram. Soc. 34 (2014) 4099–4103.
[58] J. Balko, T. Csanádi, R. Sedlák, M. Vojtko, A. Kovalčíková, K. Koval, P. Wyzga, A. Naughton-Duszová, Nanoindentation and tribology of VC, NbC and ZrC refractory carbides, J. Eur. Ceram. Soc. 37 (2017) 4371–4377.
[59] C.J. Smith, X.X. Yu, Q. Guo, C.R. Weinberger, G.B. Thompson, Phase, hardness, and deformation slip behavior in mixed HfxTa1-xC, Acta Mater. 145 (2018) 142–153.
[60] S.R. Bakshi, V. Musaramthota, D. Lahiri, V. Singh, S. Seal, A. Agarwal, Spark plasma sintered tantalum carbide: effect of pressure and nano-boron carbide addition on microstructure and mechanical properties, Mater. Sci. Eng. A 528 (2011) 1287–1295.
[61] D.J. Rowcliffe, G.E. Hollox, Hardness anisotropy, deformation mechanisms and brittle-to-ductile transition in carbide, J. Mater. Sci. 6 (1971) 1270–1276.
[62] N. De Leon, X.X. Yu, H. Yu, C.R. Weinberger, G.B. Thompson, Bonding effects on the slip differences in the B1 monocarbides, Phys. Rev. Lett. 114 (2015) 1–5.
[63] I. Frantsevich, E. Zhurakovskii, A. Lyashchenko, Elastic constants and characteristics of the electron structure of certain classes of refractory compounds obtained by the metal-powder method, Inorg. Mater. (Engl. Transl.) 3 (1967) 6–12.
[64] A. Nino, T. Hirabara, S. Sugiyama, H. Taimatsu, Preparation and characterization of tantalum carbide (TaC) ceramics, Int. J. Refract. Metals Hard Mater. 52 (2015) 203–208.
[65] S.P. Dodd, M. Cankurtaran, B. James, Ultrasonic determination of the elastic and nonlinear acoustic properties of transition-metal carbide ceramics: TiC and TaC, J. Mater. Sci. 38 (2003) 1107–1115.
[66] X. Zhang, G.E. Hilmas, W.G. Fahrenholtz, Densification and mechanical properties of TaC-based ceramics, Mater. Sci. Eng. A 501 (2009) 37–43.
[67] W.S. Williams, R.D. Schaal, Elastic deformation, plastic flow, and dislocations in single crystals of titanium carbide, J. Appl. Phys. 33 (1962) 955–962.
[68] E. Török, J. Perry, L. Chollet, W. Sproul, Young's modulus of TiN, TiC, ZrN and HfN, Thin Solid Films 153 (1987) 37–43.
[69] J.J. Gilman, B.W. Roberts, Elastic Constants of TiC and TiB2, J. Appl. Phys. 32 (1961) 1405.
[70] L. Wang, M. Wixom, L. Thompson, Structural and mechanical properties of TiB2 and TiC prepared by self-propagating high-temperature synthesis /dynamic compaction, J. Mater. Sci. 29 (1994) 534–543.
[71] H. Doi, Y. Fujiwara, K. Miyake, Y. Oosawa, A systematic investigation of elastic moduli of WC-Co alloys, Metall. Trans. 1 (1970) 1417–1425.
[72] W. Feng, S. Cui, H. Hu, G. Zhang, Z. Lv, Electronic structure and elastic constants of TiCxN1-x, ZrxNb1-xC and HfCxN1-xalloys: a first-principles study, Phys. B Condens. Matter 406 (2011) 3631–3635.
[73] V. Krasnenko, M.G. Brik, First-principles calculations of hydrostatic pressure effects on the structural, elastic and thermodynamic properties of cubic monocarbides XC (X = Ti, V, Cr, Nb, Mo, Hf), Solid State Sci. 14 (2012) 1431–1444.
[74] X.G. Lu, M. Selleby, B. Sundman, Calculations of thermophysical properties of cubic carbides and nitrides using the Debye-Grüneisen model, Acta Mater. 55 (2007) 1215–1226.
[75] Y. Liu, Y. Jiang, R. Zhou, J. Feng, First principles study the stability and mechanical properties of MC (M = Ti, V, Zr, Nb, Hf and Ta) compounds, J. Alloys Compd. 582 (2014) 500–504.
[76] A. Zaoui, B. Bouhafs, P. Ruterana, First-principles calculations on the electronic structure of TiCxN1-x, ZrxNb1-xC and HfCxN1-xalloys, Mater. Chem. Phys. 91 (2005) 108–115.
[77] L. Chen, Q. Wang, L. Xiong, H. Gong, Mechanical properties and point defects of MC (M=Ti, Zr) from first-principles calculation, J. Alloys Compd. 747 (2018) 972–977.
[78] E. Rudy, Constitution of ternary titanium-tungsten-carbon alloys, J. Less Common Metals 33 (1973) 245–273.
[79] B. Haldar, D. Bandyopadhyay, R.C. Sharma, N. Chakraborti, The Ti-W-C (titanium-tungsten-carbon) system, J. Phase Equilibria 20 (1999) 337–343.
[80] F. Gao, Hardness of cubic solid solutions, Sci. Rep. 7 (2017) 1–6.
[81] K. Nakamura, M. Yashima, Crystal structure of NaCl-type transition metal monocarbides MC (M = V, Ti, Nb, Ta, Hf, Zr), a neutron powder diffraction study, Mater, Sci. Eng. B Solid-State Mater. Adv. Technol. 148 (2008) 69–72.